

γ -Selective Cross-Coupling Reactions of Potassium Allyltrifluoroborates with Haloarenes Catalyzed by a Pd(0)/D-*t*-BPF or Pd(0)/Josiphos ((*R,S*)-CyPF-*t*-Bu) Complex: Mechanistic Studies on Transmetalation and Enantioselection

Yasunori Yamamoto,* Shingo Takada, and Norio Miyaura*

Division of Chemical Process Engineering, Graduate School of Engineering, Hokkaido University, Sapporo 060-8628, Japan

Tetsuji Iyama and Hiroto Tachikawa

Division of Materials Chemistry, Graduate School of Engineering, Hokkaido University, Sapporo 060-8628, Japan

Received August 27, 2008

Cross-coupling between bromoarenes and [(*E*)-CH₃CH=CHCH₂BF₃]*K* (**2a**) by a catalyst prepared from Pd(OAc)₂ and D-*t*-BPF selectively provided γ -coupling products via S_E2' substitution. Mechanistic study of transmetalation revealed a heretofore unknown process, namely, formation of a highly electrophilic [Pd(Ar)(D-*t*-BPF)]⁺ before transmetalation with **2a**. Thus, kinetic data in coupling of 4-substituted bromoarenes with **2a** showed a linear positive correlation ($\rho = -1.1$) accelerated by donating substituents. This rate-determining role of transmetalation was further confirmed by kinetic data between oxidative adducts [Pd(Ar)(Br)(D-*t*-BPF)] and **2a** that exhibited an analogous correlation with a negative ρ -value (-0.50). Theoretical study by density functional theory (DFT) calculation showed that transmetalation between [Ar-Pd]⁺ and **2a** via an S_E2' (open) transition state is a slightly lower energy process than an S_E2' (closed) process. Allylic substitutions with chiral catalysts are the current topics for enantioselective C–C bond formation, but the catalysts that are effective for allylic nucleophiles have remained unexplored. Among the ligands screened, (*R,S*)-CyPF-*t*-Bu was found to achieve 77–90% ee for representative para- and meta-substituted bromoarenes and 2-bromo-1-alkenes in refluxing aqueous tetrahydrofuran (THF) or MeOH. To obtain mechanistic information on enantioselection, the mode of substrate coordination to a cationic phenylpalladium intermediate was calculated, that is, the reaction stage directly preceding the stereodetermining insertion step by DFT calculation. A stable adduct between [Pd(CyPF-*t*-Bu)(Ph)]⁺ and **2a** located at the C–C double bond from its *re*-face yielding the experimentally observed *R*-product is preferred thermodynamically rather than the corresponding *si*-coordination.

Introduction

Transition-metal-catalyzed cross-coupling reactions have proved to be one of the most powerful methods for selective C–C bond formation.¹ Among the possible combinations of electrophiles and nucleophiles, reactions of allylic metals with aryl, alkenyl, and allyl electrophiles or with their reversed combination provide an important class of compounds because of the frequent occurrence of allylic fragments in natural products.² The coupling reactions of allylmagnesium,³ -zinc,⁴ -boron,⁵ -silicon,⁶ -tin,⁷ and -zirconium⁸ compounds with Ni and Pd catalysts have been extensively studied. Perfect control of the coupling position by phosphine ligands was first achieved by Hatanaka and Hiyama et al. using a combination of

allyltrifluorosilanes and haloarenes.^{6a,c} The coupling selectively occurred at the γ -carbon when using PPh₃ or bisphosphines possessing a large bite angle such as 1,4-bis(diphenylphosphino)butane (dppb), whereas bisphosphines possessing a relatively small angle such as 1,3-bis(diphenylphosphino)propane (dppp) underwent selective coupling at the α -carbon. Such an effect of phosphine ligands was also demonstrated in regioselective Stille coupling of aryl halides with Me₃SiCH₂CH=CHCH₂-SnBu₃ at the α - or γ -carbon.^{7g} There have been very few attempts to employ allylboron compounds, but boron reagents have various advantages, including availability, air and moisture stability, low toxicity, and easy removal of boron-derived byproducts. We have reported the efficiency of potassium allyltrifluoroborates for perfect γ -selective coupling with bro-

* To whom correspondence should be addressed. Tel/fax: +81-11-706-6561; e-mail: yasuyama@eng.hokudai.ac.jp (Y.Y.) and miyaura@eng.hokudai.ac.jp.

(1) For reviews, see: (a) *Boronic Acids*; Hall, D. G., Ed.; Wiley-VCH: Weinheim, Germany, 2005. (b) *Metal-Catalyzed Cross-Coupling Reactions*, 2nd ed.; de Meijere, A., Diederich, F., Eds.; Wiley-VCH: Weinheim, Germany, 2004. (c) *Cross-Coupling Reactions. A Practical Guide*; Miyaura, N., Ed.; Springer: Berlin, 2002. (d) *Handbook of Organopalladium Chemistry for Organic Synthesis*; Negishi, E.-I., Ed.; John Wiley & Sons: New York, 2002. (e) *Metal-Catalyzed Cross-Coupling Reactions*; Diederich, F., Stang, P. J., Eds.; Wiley-VCH: Weinheim, Germany, 1998.

(2) (a) Heck, R. H. *J. Am. Chem. Soc.* **1968**, *90*, 5531. (b) Negishi, E.-I.; Chatterjee, S.; Matsushita, H. *Tetrahedron Lett.* **1981**, *22*, 3737. (c) Legros, J.-Y.; Flaud, J.-C. *Tetrahedron Lett.* **1990**, *31*, 7453. (d) Mareno-Mañas, M.; Pajuelo, F.; Pleixats, R. *J. Org. Chem.* **1995**, *60*, 2396. (e) Chung, K.-G.; Miyake, Y.; Uemura, S. *J. Chem. Soc., Perkin Trans. 1* **2000**, 2725. (f) Bouyssi, D.; Gerusz, V.; Balme, G. *Eur. J. Org. Chem.* **2002**, 2445. (g) Ikegami, R.; Koresawa, A.; Shibata, T.; Takagi, K. *J. Org. Chem.* **2003**, *68*, 2195. (h) Kayaki, Y.; Koda, T.; Ikariya, T. *Eur. J. Org. Chem.* **2004**, 4989. (i) Tsukamoto, H.; Sato, M.; Kondo, Y. *Chem. Commun.* **2004**, 1200.

Table 1. γ -Selective Coupling of Potassium Allyltrifluoroborates (**2**) with Haloarenes Giving **3** (Scheme 1)

entry	2	ArBr, X =	ligand	yield/% ^a (3/4)
1 ^b	2a	4-MeO	PPh ₃	42 (78/22)
2 ^b	2a	4-MeO	dppm	35 (78/22)
3 ^b	2a	4-MeO	dppe	17 (37/63)
4 ^b	2a	4-MeO	dppp	37 (>99/1)
5 ^b	2a	4-MeO	dppf	68 (>99/1)
6 ^b	2a	4-MeO	DPEphos	21 (>99/1)
7 ^b	2a	4-MeO	Xantphos	10 (>99/1)
8 ^b	2a	4-MeO	DBFphos	10 (>99/1)
9 ^b	2a	4-MeO	D- <i>t</i> -BPF	87 (>99/1)
10 ^c	2a	4-MeO	D- <i>t</i> -BPF	85 (>99/1)
11 ^c	2a	4-CO ₂ Me	D- <i>t</i> -BPF	99 (>99/1)
12 ^c	2b	4-CO ₂ Me	D- <i>t</i> -BPF	91 (>99/1)
13 ^c	2c	4-CO ₂ Me	D- <i>t</i> -BPF	99 (>99/1)
14 ^c	2d	4-CO ₂ Me	D- <i>t</i> -BPF	96 (>99/1)
15 ^c	2e	4-CO ₂ Me	D- <i>t</i> -BPF	99 (>99/1)
16 ^{c,d}	2f	4-CO ₂ Me	D- <i>t</i> -BPF	99 (-)
17 ^c	2g	4-CO ₂ Me	D- <i>t</i> -BPF	99 (<1/99) ^e

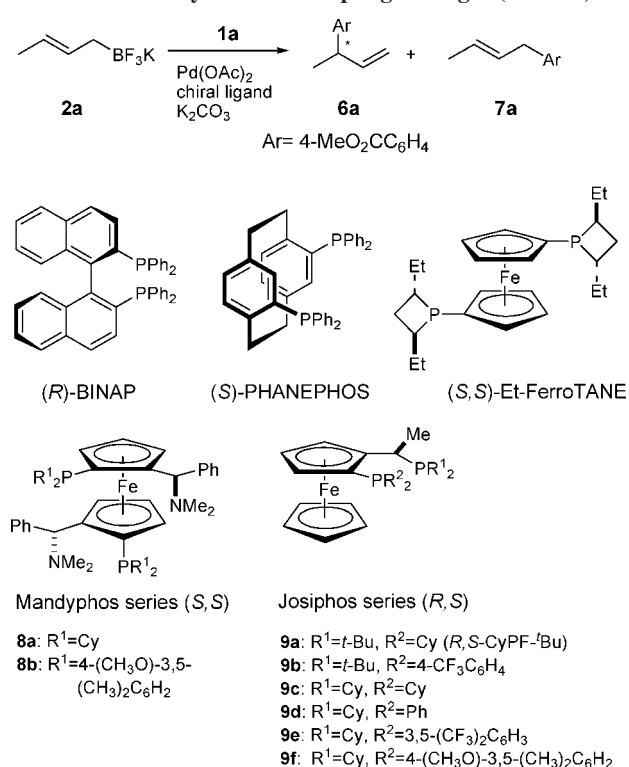
^a NMR yields for entries 1–8 and isolated yields for entries 9–17.

^b The reactions were conducted for 20 h at reflux in THF–H₂O (10/1) in the presence of Pd(OAc)₂ (3 mol %), a ligand (3 mol %), haloarene (0.5 mmol), **2** (0.75 mmol), and K₂CO₃ (1.5 mmol). ^c The reactions were conducted for 22 h at reflux in THF in the presence of Pd(OAc)₂ (3 mol %), a ligand (3.6 mol %), haloarene (1 mmol), **2** (2.5 mmol), and K₂CO₃ (3 mmol). ^d Walphos was used as ligand. ^e E/Z = 55/45.

and 1-methyl-2-propenylboronate (**2g**). Among these boronates chosen for investigating scope and limitations, it was interesting that **2d** and **2e** selectively gave a quaternary carbon (entries 14 and 15) and **2g** gave a linear 2-butenyl product via complete S_E2' substitution (entry 17). Our previous study also showed that other representative bromoarenes, including hindered 2,6-dimethyl derivatives and 2-bromo-1-alkenes, achieve γ -selectivities higher than 99%.⁹ Thus, such high yields and high γ -selectivity are characteristic for D-*t*-BPF, which has a large bite angle and steric hindrance and a strong electron-donating ability to the palladium(0) metal center.

Asymmetric Coupling Catalyzed by Pd(0)/(R,S)-CyPF-*t*-Bu. Transition-metal-catalyzed allylic substitutions with nucleophiles, especially their asymmetric versions using chiral catalysts, are the current topics.^{17–19} Several efficient chiral catalysts have been developed for those purposes and have considerably expanded the scope of enantioselective C–C and C–heteroatom bond formation. However, chiral catalysts for allylic nucleophiles have remained unexplored.

The regioselectivities of the coupling position (**6a**, **7a**) and enantioselectivities of **6a** were highly sensitive to phosphine ligands employed for palladium acetate in the reaction between potassium (*E*)-crotyltrifluoroborate (**2a**) and methyl 4-bromobenzoate (Scheme 2 and Table 2). The use of BINAP, Et-FerroTANE, PHANEPHOS, and other representative C₂ symmetric chiral phosphines resulted in the formation of two isomers

Scheme 2. Asymmetric Coupling Giving **6** (Table 2)**Table 2.** Asymmetric Coupling of Potassium Crotyltrifluoroborate (**2a**) with Methyl 4-Bromobenzoate (**1a**) (Scheme 2)^a

entry	ligand	yield/% ^b	6a/7a	% ee of 6a ^c
1	(<i>R</i>)-BINAP	86	68/32	3
2	(<i>S,S</i>)-Et-FerroTANE	84	31/69	12
3	(<i>S</i>)-PHANEPHOS	63	84/16	20 (<i>S</i>)
4	8a	98	93/7	31 (<i>R</i>)
5	8b	84	96/4	46 (<i>S</i>)
6	9a ((<i>R,S</i>)-CyPF- <i>t</i> -Bu)	96	92/8	63 (<i>R</i>)
7	9b	54	83/17	26 (<i>R</i>)
8	9c	73	99/1	10
9	9d	57	83/17	44 (<i>R</i>)
10	9e	64	14/86	5
11	9f	63	21/79	4
12 ^d	9a ((<i>R,S</i>)-CyPF- <i>t</i> -Bu)	93	95/5	82 (<i>R</i>)
13 ^e	9a ((<i>R,S</i>)-CyPF- <i>t</i> -Bu)	93	93/7	82 (<i>R</i>)

^a The reactions were conducted at reflux for 22 h in THF in the presence of Pd(OAc)₂ (3 mol %), a ligand (3.6 mol %), methyl 4-bromobenzoate (1 mmol), **2a** (2.5 mmol), and K₂CO₃ (3 mmol).

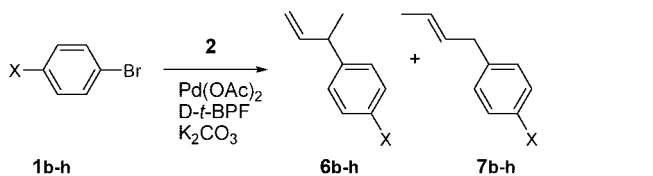
^b Isolated yields. ^c Enantiomer excess was determined by a chiral stationary column. ^d The reaction in THF–H₂O (1/4). ^e The reaction in MeOH–H₂O (1/9).

with low enantioselectivities (entries 1–3). On the other hand, the use of ferrocene-type ligands of Mandypfos and Josiphos series (**8** and **9**) is dominated by the formation of a γ -coupling product (**6**) (entries 4–11). Among the ligands screened, (*R,S*)-CyPF-*t*-Bu (**9a**) was finally found to be the best ligand to achieve 63% ee with 92% γ -selectivity in refluxing THF (entry 6). The absolute configuration of 3-(4-methoxycarbonylphenyl)-1-butene (**6a**) was established to be *R* ([α]_D – 12.68 (*c* 0.59, benzene)) by the specific rotation reported for (*S*)-isomer ([α]_D + 12 (*c* 0.9, CHCl₃)) and retention times of two enantiomers in high-performance liquid chromatography (HPLC) analysis.^{18d,19b} Allyltrifluoroborates (**2**) are highly insoluble in common organic solvents. Thus, addition of water to THF or MeOH resulted in significant improvement of yields and enantioselectivities because of the high solubility of **2a** in aqueous solvents (entries 12 and 13). The enantioselectivities thus achieved were in the

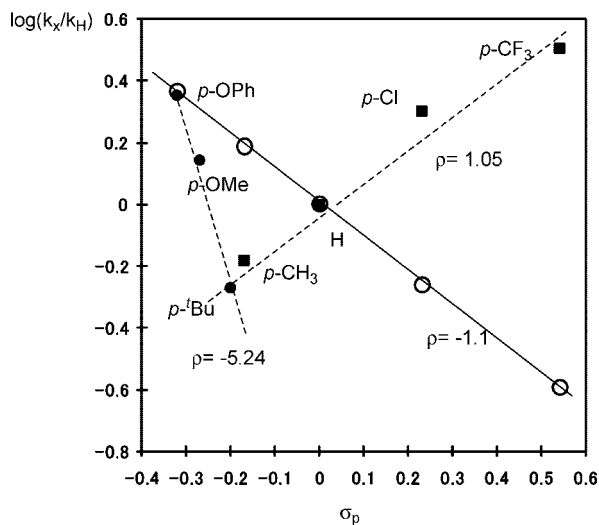
(17) (a) Hayashi, T. *J. Organomet. Chem.* **2002**, 653, 41. (b) Hayashi, T.; Tajika, M.; Tamao, K.; Kumada, M. *J. Am. Chem. Soc.* **1976**, 98, 3718. (c) Hayashi, T.; Konishi, M.; Fukushima, M.; Mise, T.; Kagotani, M.; Tajika, M.; Kumada, M. *J. Am. Chem. Soc.* **1982**, 104, 180. (d) Hayashi, T.; Konishi, M.; Fukushima, M.; Kanehira, K.; Hioki, T.; Kumada, M. *J. Org. Chem.* **1983**, 48, 2195.

(18) (a) van Zijl, A. W.; Arnold, L. A.; Minnaard, A. J.; Feringa, B. L. *Adv. Synth. Catal.* **2004**, 346, 413. (b) Tissot-Croset, K.; Alexakis, A. *Tetrahedron Lett.* **2004**, 45, 7375. (c) Yorimitsu, H.; Oshima, K. *Angew. Chem., Int. Ed.* **2005**, 44, 4435. (d) López, F.; van Zijl, A. W.; Minnaard, A. J.; Feringa, B. L. *Chem. Commun.* **2006**, 409.

(19) (a) RajanBabu, T. V.; Nomura, N.; Nandi, J. J. M.; Park, H.; Sun, X. *J. Org. Chem.* **2003**, 68, 8431. (b) Zhang, A.; RajanBabu, T. V. *Org. Lett.* **2004**, 6, 1515. (c) Park, H.; Kumareswaran, R.; RajanBabu, T. V. *Tetrahedron* **2005**, 61, 6352. (d) Shi, W.-J.; Xie, J.-H.; Zhou, Q.-L. *Tetrahedron: Asymmetry* **2006**, 16, 705.

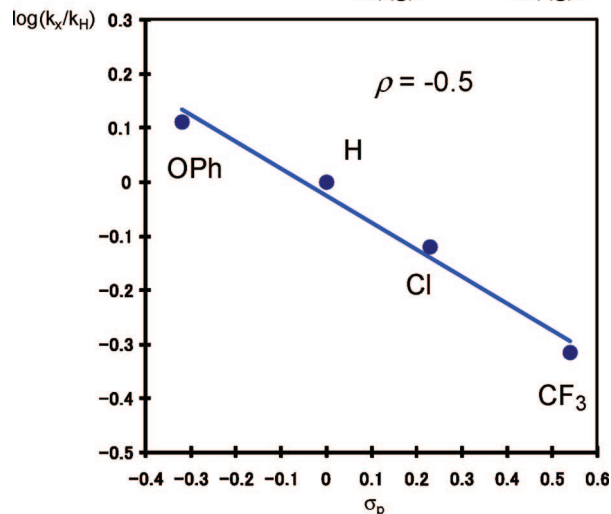
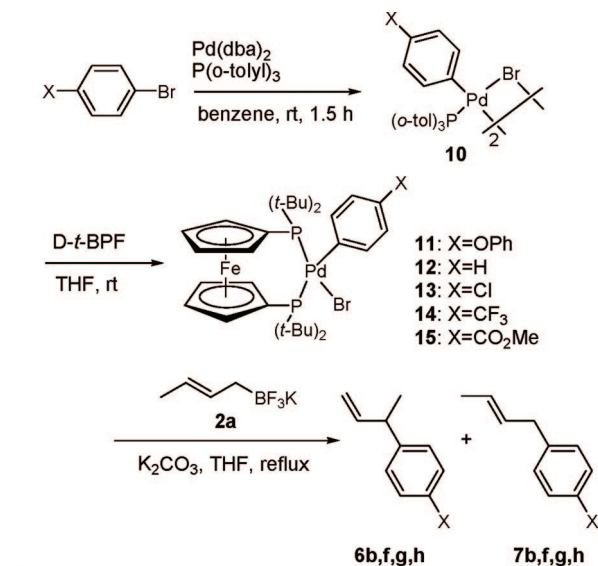
Scheme 3. Hammett Plot Based on Kinetic Data and σ Values in the Reaction between 1 and 2

b: X=OPh, c: X=OMe, d: X=Me, e: X= *t*-Bu, f: X= H, g: X= Cl, h: X= CF₃



range of 77–90% ee for representative para- and meta-substituted bromoarenes and 2-bromo-1-alkenes.¹⁰

Kinetic Studies on Transmetalation. The reaction between **2a** and para-substituted bromoarenes with Pd(OAc)₂/D-*t*-BPF in refluxing THF showed Hammett's correlations suggesting a rate-determining role of the transmetalation step (Scheme 3). There were two correlations when the relative rates were estimated by a competitive reaction of two bromoarenes for **2a** (dotted lines, ● and ■). The reactivity linearly was increased by donating groups having σ -values lower than -0.1 (●, $\rho = -5.24$) and withdrawing groups higher than 4-MeOC₆H₄Br (■, $\rho = 1.05$). This result was in sharp contrast to the single correlation ($\rho = -1.1$) to σ in a range of -0.3 to 0.5 when the initial rates were estimated by conversions of the independent runs for each bromoarene (solid line, ○). Among the steps involved in the catalytic cycle of cross-coupling, oxidative addition exhibits a linear positive correlation accelerated by withdrawing groups as was observed in most cross-coupling reactions of arylboronic acids with haloarenes.²⁰ It is difficult to conclude that this is due to the rate-determining role of reductive elimination²¹ because there is no scrambling of the coupling position between γ -coupling products and thermally stable linear α -carbon coupling products. Thus, it is reasonable to conclude that the two correlations shown by the dotted lines were the result of a balance of the reverse effects of substituents on oxidative addition and transmetalation. The linear correlation

Scheme 4. Hammett Plot Based on Kinetic Data and σ Values in the Coupling between 11–15 and 2a

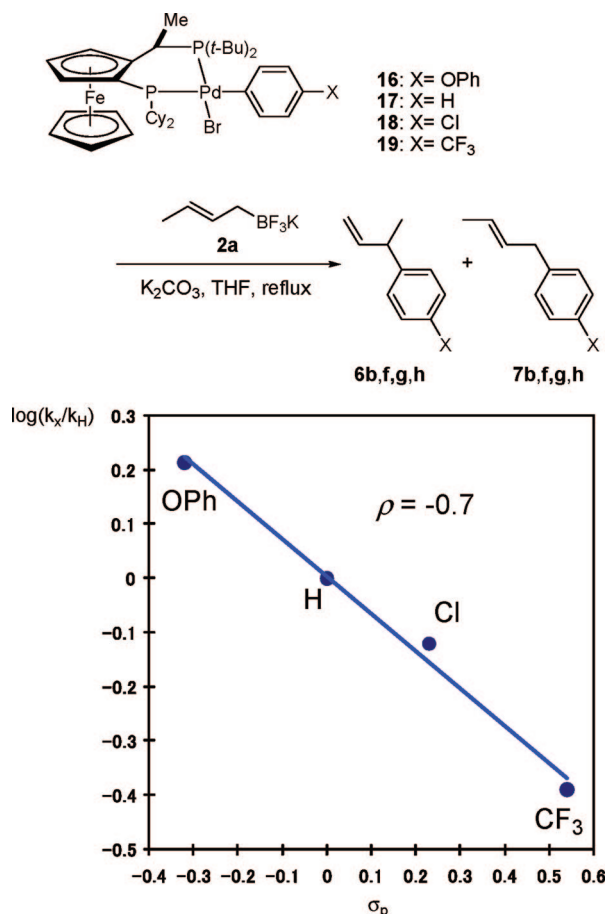
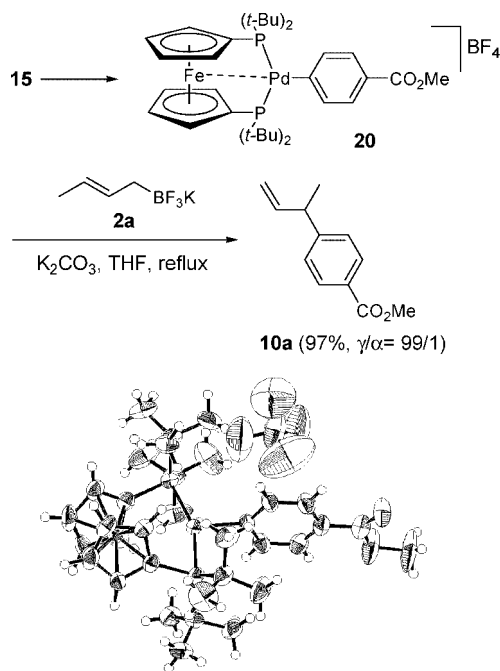
shown by a solid line is attributable to the electronic effect on transmetalation.

Five oxidative adducts of bromoarenes, **11–15** (X = OPh, H, Cl, CF₃, CO₂Me), were synthesized by the method of Hartwig and co-workers²² as intermediates for transmetalation. The competitive reaction of (*E*)-crotylboronate (**2a**) with two oxidative adducts (**11–14**) in refluxing THF showed a single correlation with a small negative ρ -value (-0.50) (Scheme 4). The CyPF-*t*-Bu ligand used for asymmetric coupling is also dominated by the γ -coupling products for formation of a chiral secondary carbon. The reaction between (*E*)-crotylboronate (**2a**) and four oxidative adducts (**16–19**, X = OPh, H, Cl, CF₃) of CyPF-*t*-Bu showed a single correlation with a small negative ρ -value (Scheme 5). The slope (-0.70) was almost the same as that of D-*t*-BPF ligand.

A possible mechanism that accounts for the electronic effect of substituents is one proceeding through a cationic palladium(II) species by elimination of a bromine ligand before reaction with **2a**. The expected cationic palladium(II) species (**20**) was synthesized by treatment of **15** with AgBF₄.^{22b} Indeed, the reaction between **2a** and **20** afforded perfect γ -selectivity (Scheme 6). The equilibrium formation of [Pd(Ar)(D-*t*-BPF)]⁺ from Pd(Ar)(D-*t*-BPF)(Br) has been reported.^{22b}

(20) (a) Moriya, T.; Miyaura, N.; Suzuki, A. *Synlett* **1994**, 149. (b) Saito, S.; Oh-tani, S.; Miyaura, N. *J. Org. Chem.* **1997**, *62*, 8024. (c) Weissman, H.; Milstein, D. *Chem. Commun.* **1999**, 1901. (d) Zim, D.; Lando, V. R.; Dupont, J.; Montiro, A. L. *Org. Lett.* **2001**, *3*, 3049. (e) Liang, L.-C.; Chien, P.-S.; Huang, M.-H. *Organometallics* **2005**, *24*, 353.

(21) (a) Temple, J. S.; Riediker, M.; Schwartz, J. *J. Am. Chem. Soc.* **1982**, *104*, 1310. (b) Goliaszewski, A.; Schwartz, J. *J. Am. Chem. Soc.* **1984**, *106*, 5028. (c) Goliaszewski, A.; Schwartz, J. *Organometallics* **1985**, *4*, 417. (d) Bertani, R.; Berton, A.; Carturan, G.; Campostrini, R. *J. Organomet. Chem.* **1988**, *349*, 263.

Scheme 5. Hammett Plot Based on Kinetic Data and σ Values in the Reaction between 16–19 and 2a**Scheme 6. A Regiochemical Selectivity in the Coupling of Cationic Complex (20) with 2a**

ORTEP drawing of (D-*t*-BPF)Pd(4-MeO₂CC₆H₄)(BF₄) (20)

Density Functional Theory (DFT) Calculations on the Energy Diagram of Oxidative Addition, Transmetalation, and Reductive Elimination Reactions. Results of theoretical studies on oxidative addition and reductive elimination of cross-

coupling reaction and Heck coupling reaction have been reported.^{23–27} The energy diagram of oxidative addition, Pd(PH₃)₂ (a) + Ph–Br (b) → TS_{oa} → Pd(PH₃)₂(Ph)(Br) (c), is given in Figure 1, while the structure of the transition state (TS_{oa}) is illustrated in Figure 2. The C–Br length of Ph–Br (b) at the initial separation is calculated to be 1.973 Å. At the transition state, the C–Br length of TS_{oa} is 2.239 Å, which is elongated by 0.266 Å by the interaction with Pd. TS_{oa} has a triangle form composed of a Br–Pd–Ph skeleton with an angle of 52.3° (∠Br–Pd–C). The bond lengths of Pd–Br and Pd–C of TS_{oa} are 2.774 and 2.136 Å, respectively. The activation energy at TS_{oa} is 10.2 kcal/mol relative to the initial separation (zero level) at the B3LYP/LANL2DZ level. The oxidative adduct, Pd(PH₃)₂(Ph)(Br), is 26.1 kcal/mol lower in energy than that of the initial separation, Pd(PH₃)₂ + Ph–Br. If the solvent effect is not considered, the energy level of c is slightly larger than that in THF (–21.2 kcal/mol). The formation of a cationic palladium(II) species (d) via substitution of the Pd–Br bond with H₂O takes place smoothly with a 13.6 kcal/mol energy barrier, whereas it is significantly large (100.4 kcal/mol) in the absence of a solvent effect indicating an important role of the solvent effect in this charge-separated system. The energy level of this state composed of (H₃P)Pd(Ph)⁺–OH₂ (d) and CH₃CH=CHCH₂BF₃[–] (e) is –12.6 kcal/mol lower than that of the initial state. The coordination of allylboronate (e) to a cationic palladium(II) complex (d) by the S_E2' (closed) transition state (f) is +2.0 kcal/mol higher than that by the S_E2' (open) state (g), though the former state (f', 10.4 kcal/mol) is 8 kcal/mol lower than the latter one (g', +18.4 kcal/mol) in the absence of a solvent effect. Thus, there is no large difference in energy levels between S_E2' closed and open coordination, whereas the S_E2' open process is slightly more stable than the S_E2' closed process in THF solvent. After TS_{tm}, the BF₃ group is substituted by a water molecule for formation of a strong Pd–C bond (h) with a 30 kcal/mol energy barrier. The structure of the transition state for transmetalation (TS_{tm}) is illustrated in Figure 2. If the solvent effect is not considered, the energy level of h becomes higher than zero level (+16.9 kcal/mol). The transition state of reductive elimination (TS_{re}) has a triangle structure composed of Pd and two carbon atoms of phenyl and allyl groups as shown in Figure 2. The energy of TS_{re} is 16.3 kcal/mol higher than

(22) (a) Paul, F.; Patt, J.; Hartwig, J. F. *Organometallics* **1995**, *14*, 3030. (b) Mann, G.; Shelby, Q.; Roy, A. H.; Hartwig, J. F. *Organometallics* **2003**, *22*, 2775.

(23) (a) Sumimoto, M.; Iwane, N.; Takahama, T.; Sakaki, S. *J. Am. Chem. Soc.* **2004**, *126*, 10457. (b) Braga, A. A.; Morgon, N. H.; Ujaque, G.; Maseras, F. *J. Am. Chem. Soc.* **2005**, *127*, 9298. (c) Goossen, L. J.; Koley, D.; Hermann, H. L.; Thiel, W. *J. Am. Chem. Soc.* **2005**, *127*, 11102. (d) Goossen, L. J.; Koley, D.; Hermann, H. L.; Thiel, W. *Organometallics* **2006**, *25*, 54. (e) Braga, A. A.; Ujaque, G.; Maseras, F. *Organometallics* **2006**, *25*, 3647. (f) Baraga, A. A. C.; Morgon, N. H.; Ujaque, G.; Lledós, A.; Maseras, F. *J. Organomet. Chem.* **2006**, *691*, 4459. (g) Sicre, C.; Braga, A. A. C.; Maseras, F.; Cid, M. M. *Tetrahedron* **2008**, *64*, 7437. (h) Huang, Y.-L.; Weng, C.-M.; Hong, F.-E. *Chem. Eur. J.* **2008**, *14*, 4426.

(24) (a) Goossen, L. J.; Koley, D.; Hermann, H. L.; Thiel, W. *Organometallics* **2005**, *24*, 2398. (b) Ahlquist, M.; Norrby, P.-O. *Organometallics* **2007**, *26*, 550. (c) Lam, K. C.; Marder, T. B.; Lin, Z. *Organometallics* **2007**, *26*, 758. (d) Fazaeli, R.; Ariafard, A.; Jamshidi, S.; Tabatabaie, E. S.; Pishro, K. A. *J. Organomet. Chem.* **2007**, *692*, 3984. (e) Li, Z.; Guo, Q.-X.; Liu, L. *Organometallics* **2008**, *27*, 4043.

(25) (a) Ananikov, V. P.; Musaev, D. G.; Morokuma, K. *J. Am. Chem. Soc.* **2002**, *124*, 2839. (b) Cárdenas, D. J.; Echavarran, A. M. *New J. Chem.* **2004**, *28*, 338. (c) Ananikov, V. P.; Musaev, D. G.; Morokuma, K. *Eur. J. Inorg. Chem.* **2007**, 5390.

(26) (a) Lee, M.-T.; Lee, H. M.; Hu, C.-H. *Organometallics* **2007**, *26*, 1317. (b) Surawatanawong, P.; Fan, Y.; Hall, M. B. *J. Organomet. Chem.* **2008**, *693*, 1552.

(27) (a) Nova, A.; Ujaque, G.; Maseras, F.; Lledós, A.; Espinet, P. *J. Am. Chem. Soc.* **2006**, *128*, 14571. (b) Álvarez, R.; Pérez, M.; Faza, O. N.; de Lera, A. R. *Organometallics* **2008**, *27*, 3378.

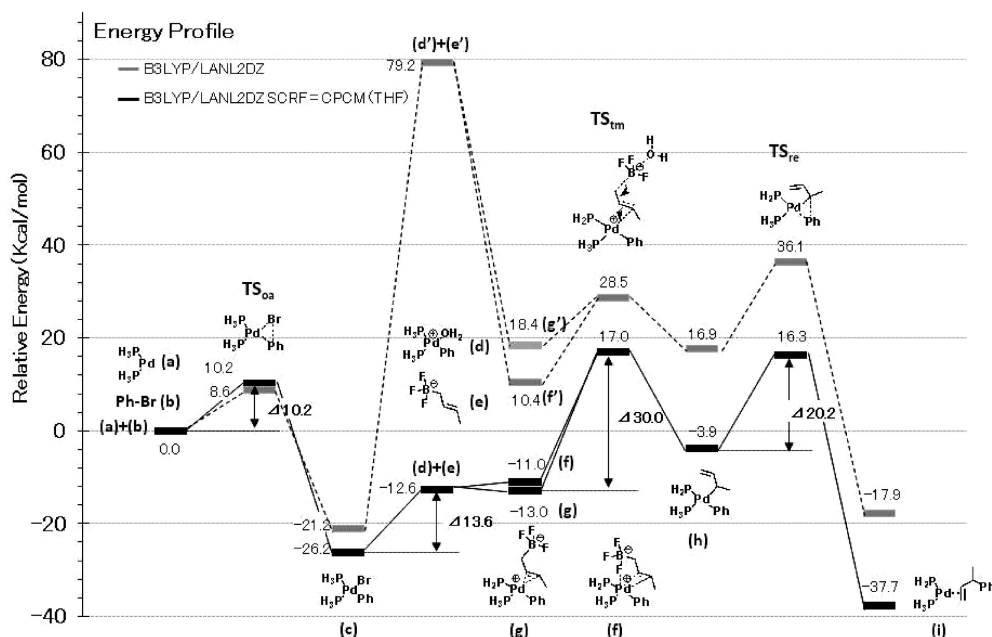


Figure 1. DFT calculation of transition state.

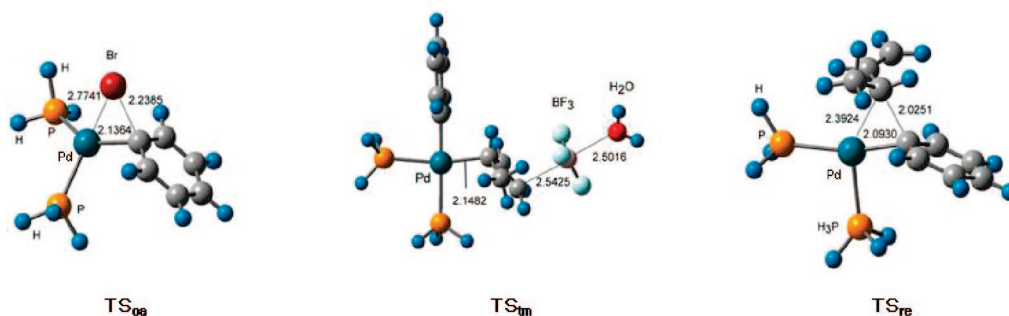


Figure 2. Optimized structures of TS_{oa} , TS_{tm} , and TS_{re} calculated at the B3LYP/LANL2DZ level.

zero level. In the final state for giving **i**, the bonding of the phenyl group (Ph) is changed from Pd to the carbon atom of allylic carbon, and the Pd atom interacts with the C=C double bond of $H_2C=CH(Ph)CH_3$ (**i**). The reaction energy is calculated to be -37.7 kcal/mol, which is large enough to proceed under thermal conditions.

Proposed Mechanism for Transmetalation. Transmetalation is a critical process involved in various metal-catalyzed bond-forming reactions, but the mechanistic features, including its kinetics, still remain unexplored. Intermediates before transmetalation between arylboronic acids and platinum(II) halides or palladium(II) halides were studied by Osakada²⁸ and Hartwig.²⁹ We reported the results of a kinetic study of transmetalation between para-substituted arylboronic acids and cationic $[Pd(Ph)(PPh_3)(dppe)]BF_4$ that showed a small negative ρ value (-0.54).³⁰ There have also been theoretical studies on transmetalation of arylboronic acids and diborons.²³ Among precedents for transmetalation between $Ar-Pd-X$ and allylfluorosilanes, an S_E2' (open) process involving a direct

interaction of the palladium metal center to the C–C double bond and an S_E2' (closed) process involving an F-chelation between Pd and Si atoms were proposed on the basis of the effects of phosphine ligands, the effect of F bases on α - and γ -coupling selectivity, and the stereochemistry in substitution of chiral allylsilane compounds.^{6b} On the other hand, the high-efficiency cationic palladium species for transmetalation has been demonstrated in the palladium-catalyzed bond-forming reactions of $ArB(OH)_2$ with ArN_2BF_4 or Ar_2IX ($X = BF_4, OTf$)³¹ and conjugate addition reactions of arylboronic acids to enones catalyzed by dicationic $[Pd(dppe)(PhCN)_2](BF_4)_2$.³⁰ The involvement of such a cationic species in Heck reaction between aryl triflates and 4-substituted styrenes was demonstrated by a kinetic study of substituents;³² however, it is not common in analogous coupling or addition reactions of organic halides.

All kinetic data suggested the formation of a cationic species (**22**) as the intermediate for transmetalation with allylborates

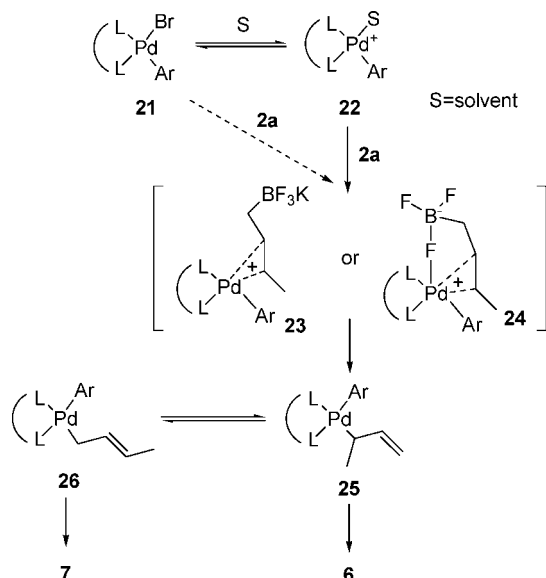
(28) (a) Osakada, K.; Onodera, H.; Nishihara, Y. *Organometallics* **2005**, *24*, 190. (b) Pantcheva, I.; Nishihara, Y.; Osakada, K. *Organometallics* **2005**, *24*, 3815. (c) Pantcheva, I.; Osakada, K. *Organometallics* **2006**, *25*, 1735. (d) Suzuki, Y.; Osakada, K. *Organometallics* **2006**, *25*, 3251.

(29) Stambuli, J. P.; Bühl, M.; Hartwig, J. F. *J. Am. Chem. Soc.* **2002**, *124*, 9346.

(30) Nishikata, T.; Yamamoto, Y.; Miyaura, N. *Organometallics* **2004**, *23*, 4317.

(31) (a) Kang, S.-K.; Lee, H.-W.; Jang, S.-B.; Ho, P.-S. *J. Org. Chem.* **1996**, *61*, 4720. (b) Sengupta, S.; Bhattacharyya, S. *J. Org. Chem.* **1997**, *62*, 3405. (c) Andrus, M. B.; Song, C. *Org. Lett.* **2001**, *3*, 3761. (d) Selvakumar, K.; Zapf, A.; Spanenberg, A.; Beller, M. *Chem. Eur. J.* **2002**, *8*, 3901. (e) Dai, M.; Liang, B.; Wang, C.; Chen, J.; Yang, Z. *Org. Lett.* **2004**, *6*, 221.

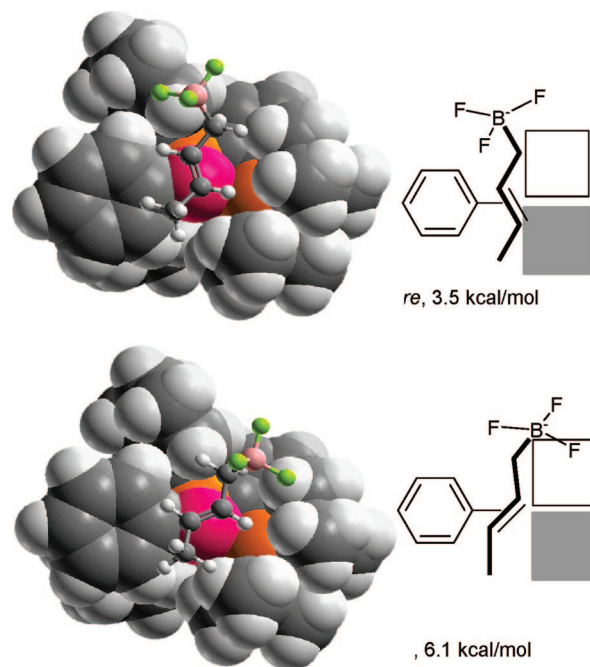
(32) (a) Ozawa, F.; Kubo, A.; Hayashi, T. *J. Am. Chem. Soc.* **1991**, *113*, 1417. (b) Cabri, W.; Candiani, I.; DeBernardinis, S.; Francalanci, F.; Penco, S. *J. Org. Chem.* **1991**, *56*, 5796. (c) Ozawa, F.; Kubo, A.; Matsumoto, Y.; Hayashi, T. *Organometallics* **1993**, *12*, 4188.

Scheme 7. Formation of a Cationic Palladium(II) Species (22) before Transmetalation with 2a

(2) when bulky and donating *D-t*-BPF was used as the ligand (Scheme 7). Since the reaction resulted in perfect γ -selectivities for all bromoarenes, the formation of an allylic π -complex intermediate before reductive elimination or an addition–elimination mechanism between Ar–Pd–X and the double bond of **2a** is ruled out. On the basis of these mechanistic precedents, our kinetic and theoretical calculation results, it was concluded that the formation of a π -complex (**23**) via coordination of the C–C double bond of **2a** to **22** is the most probable transition state that selectively gives γ -coupling products (**6**) via σ -allylpalladium(II) intermediates (**25**). A chelated cyclic complex (**24**) via coordination of F and a C–C double bond is another probable process, but the theoretical study indicated that the F chelation does not affect the stability of the transition state.

Enantioselection Mechanism in Asymmetric Coupling. The X-ray structure of [Pd(CyPF-*t*-Bu)(4-MeOC₆H₄)(NH₃)]OTf (**27**) reported by Shen and Hartwig is shown in Figure 3.³³ The molecular structure displays a slightly twisted square-planar coordination geometry for the palladium(II) atom ligated with two phosphorus atoms of (*R,S*)-CyPF-*t*-Bu, one carbon atom of the 4-methoxyphenyl group and one nitrogen atom of NH₃. There is a steric hindrance to pressure the right NH₃ upward and the left 4-methoxyphenyl group downward with respect to the P–Pd–P plane thus suggesting that the free space is accessible to reactants in the upper-right and lower-left quadrants. The dihedral angle between the P–Pd–P and C–Pd–N plane is 18.9° with anticlockwise rotation to the C–Pd–N plane. Such twisted structures suggesting free spaces accessible to the reactants have been reported for PdCl₂[(*R*)-binap]^{32c} and [Pd(PhCN)₂(chiraphos)](BF₄)₂³⁴ complexes.

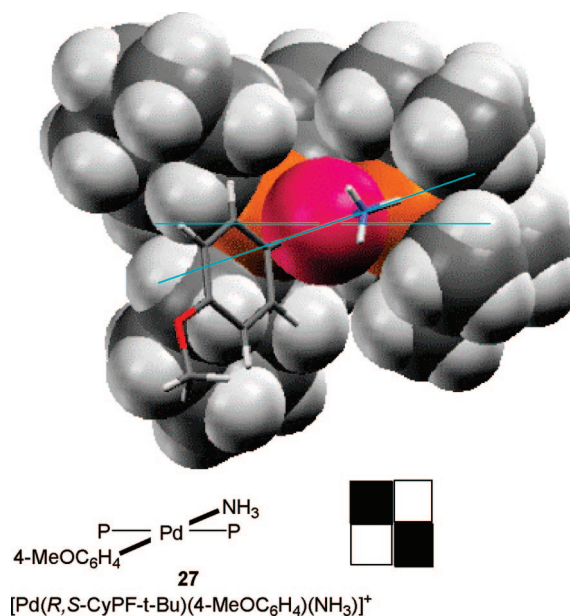
The minimum energy mode of substrate coordination to the cationic phenylpalladium intermediate was calculated, that is, the reaction stage directly preceding the stereodetermining insertion step by DFT calculation at the B3LYP/LANL2DZ level of theory. Two stable adducts between [Pd(CyPF-*t*-Bu)(Ph)]⁺ and **2a** located at the C–C double bond from its *re*-face (**28**) or *si*-face (**29**) via the S_E2' (open) process without F-chelation are shown in Scheme 8. Thus, reaction from the *re*-face yielding

Scheme 8. DFT Calculation of S_E2 (Open) Conformation at Minimum Energy Level

the experimentally observed enantiomer *R*-product is preferred thermodynamically (2.6 kcal/mol) over that of the *si*-face because of steric requirement between the methyl group of allylic moiety and the *t*-butyl group in the lower-right second quadrant. This is consistent with the experimental results shown in Table 2 suggesting a small energy difference (1–2 kcal/mol) between the two processes giving *R*- and *S*-enantiomers.

Experimental Section

General Procedure for γ -Selective Cross-Coupling (Table 1). A 20 mL flask charged with palladium acetate (0.015 mmol, 3 mol %), 1,1'-bis(di-*tert*-butylphosphino)ferrocene (*D-t*-BPF) (0.018 mmol), potassium allyltrifluoroborates (1.25 mmol), and K₂CO₃ (1.5

**Figure 3.** X-Ray structure of [Pd(*R,S*-CyPF-*t*-Bu)(4-MeOC₆H₄)(NH₃)]⁺ reported by Shen and Hartwig and possible free space accessible to reactants.(33) Shen, Q.; Hartwig, J. F. *J. Am. Chem. Soc.* **2006**, *128*, 10028.(34) Nishikata, T.; Yamamoto, Y.; Gridnev, I. D.; Miyaura, N. *Organometallics* **2005**, *24*, 5025.

mmol) was flush with nitrogen. THF (5 mL) and bromoarene (0.5 mmol) were added successively. After being refluxed for 22 h, the reaction mixture was treated with 1 N HCl (10 mL) at room temperature. Flash chromatography on silica gel gave the coupling product.

General Procedure for Asymmetric Cross-Coupling (Table 2). A flask charged with potassium (*E*)-2-butenyltrifluoroborate (2.5 mmol), Pd(OAc)₂ (3 mol %), 1-dicyclohexylphosphino-2-di-*tert*-butylphosphinoethylferrocene (CyPF-*t*-Bu) (3.6 mol %), and K₂CO₃ (3.0 mmol) was flushed with nitrogen. H₂O/MeOH (9/1, 5 mL) and bromoarene (1.0 mmol) were then added. The resulting mixture was stirred at 80 °C for 22 h. Isolated yields determined by chromatography on silica gel are shown in Table 2. Enantiomer excess was determined by a chiral stationary column.

Preparation of Palladium Complexes (Schemes 4 and 5). Pd₂(dba)₃·CHCl₃,³⁵ Pd[P(*o*-tolyl)₃]₂,³⁶ {Pd[P(*o*-tolyl)₃](Ph)(*μ*-Br)}₂,³⁶ (D-*t*-BPF)Pd(Ar)(Br) (Ar = C₆H₄-4-OPh (**11**), C₆H₅ (**12**), C₆H₄-4-Cl (**13**), C₆H₄-4-CF₃ (**14**), C₆H₄-4-CO₂Me (**15**)),^{22b} (CyPF-*t*-Bu)Pd(Ar)(Br) (Ar = C₆H₄-4-Oph (**16**), C₆H₅ (**17**), C₆H₄-4-Cl (**18**), C₆H₄-4-CF₃ (**19**)),³⁷ and [(D-*t*-BPF)Pd(C₆H₄-4-CO₂Me)](BF₄) (**20**)^{22b} were prepared according to published methods.

Pd(D-*t*-BPF)(Br)(4-PhOC₆H₄) (11**).** Crystallization from benzene/CH₂Cl₂/pentane; ¹H NMR (400 MHz, CDCl₃) δ 7.75 (d, *J* = 15.9 Hz, 1H), 7.54 (d, *J* = 8.0 Hz, 1H), 7.43–7.36 (m, 3H), 7.33 (t, *J* = 8.0 Hz, 1H), 7.10 (d, *J* = 15.9 Hz, 1H), 6.96 (d, *J* = 7.1 Hz, 2H), 5.57 (s, 4H), 4.33 (s, 4H), 1.42 (d, *J* = 7.1 Hz, 18H), 1.40 (d, *J* = 8.0 Hz, 18H); ³¹P NMR (162 MHz, CDCl₃) δ 23.75; HRMS *m/z*: calcd for C₃₈H₅₃FeO₂Pd 749.1956, found 749.1960.

Pd(D-*t*-BPF)(Br)(C₆H₅) (12**).** Crystallization from benzene/CH₂Cl₂/pentane; ¹H NMR (400 MHz, CDCl₃) δ 7.59 (d, *J* = 7.8 Hz, 2H), 7.16 (d, *J* = 7.4 Hz, 2H), 6.99 (t, *J* = 7.1 Hz, 1H), 5.54 (s, 4H), 4.33 (s, 4H), 1.40 (d, *J* = 7.4 Hz, 18H), 1.39 (d, *J* = 7.8 Hz, 18H); ³¹P NMR (162 MHz, CDCl₃) δ 20.71; HRMS *m/z*: calcd for C₃₂H₄₉FeP₂Pd 657.1694, found 657.1697; anal. calcd for C₃₃H₄₉FeP₂Pd: C, 52.09; H, 6.69; found: 48.73; H, 6.82.

Pd(D-*t*-BPF)(Br)(4-ClC₆H₄) (13**).** Crystallization from benzene/CH₂Cl₂/pentane; ¹H NMR (400 MHz, CDCl₃) δ 7.55 (d, *J* = 7.6 Hz, 2H), 7.19 (d, *J* = 7.1 Hz, 2H), 5.59 (s, 4H), 4.31 (s, 4H), 1.40 (d, *J* = 7.5 Hz, 18H), 1.38 (d, *J* = 7.6 Hz, 18H); ³¹P NMR (162 MHz, CDCl₃) δ 23.43; HRMS *m/z*: calcd for C₃₂H₄₈ClFeP₂Pd 691.1304, found 691.1307.

Pd(D-*t*-BPF)(Br)(4-CF₃C₆H₄) (14**).** Crystallization from benzene/CH₂Cl₂/pentane; ¹H NMR (400 MHz, CDCl₃) δ 7.75 (d, *J* = 15.9 Hz, 2H), 7.10 (d, *J* = 15.9 Hz, 2H), 5.63 (s, 4H), 4.34 (s, 4H), 1.40 (d, *J* = 7.1 Hz, 18H), 1.38 (d, *J* = 7.1 Hz, 18H); ³¹P NMR

(162 MHz, CDCl₃) δ 23.42; HRMS *m/z*: calcd for C₃₃H₄₈F₃FeP₂Pd 725.1568, found 725.1566.

Pd(D-*t*-BPF)(Br)(4-MeO₂CC₆H₄) (15**).** Crystallization from benzene/CH₂Cl₂/pentane; ¹H NMR (400 MHz, CDCl₃) δ 7.82 (d, *J* = 8.3 Hz, 2H), 7.77 (d, *J* = 8.3 Hz, 2H), 5.63 (s, 4H), 4.34 (s, 4H), 3.92 (s, 3H), 1.40 (d, *J* = 7.8 Hz, 18H), 1.38 (d, *J* = 7.3 Hz, 18H); ³¹P NMR (162 MHz, CDCl₃): 18.99; HRMS *m/z*: calcd for C₃₄H₅₁FeO₂P₂Pd 715.1749, found 715.1746; anal. calcd for C₃₄H₅₁FeO₂P₂Pd: C, 51.31; H, 6.46; found: 49.27; H, 6.53.

Pd(CyPF-*t*-Bu)(Br)(4-PhOC₆H₄) (16**).** Crystallization from CH₂Cl₂/pentane; ¹H NMR (400 MHz, CDCl₃) δ 7.97–7.84 (m, 2H), 7.38–7.24 (m, 4H), 7.15–7.09 (m, 1H), 7.07–6.90 (m, 2H), 5.89 (br s, 1H), 4.89 (s, 1H), 4.52 (s, 1H), 4.26 (s, 5H), 3.21–3.18 (m, 1H), 1.99 (t, *J* = 7.1 Hz, 3H), 1.70 (d, *J* = 11.7 Hz, 9H), 1.19 (d, *J* = 13.1 Hz, 9H), 2.61–0.86 (m, 22H); ³¹P NMR (162 MHz, CDCl₃): 74.22 (d, *J* = 35.1 Hz), 18.26 (br s); HRMS *m/z*: calcd for C₄₄H₆₁FeO₂P₂Pd 829.2582, found 829.2593.

Pd(CyPF-*t*-Bu)(Br)(C₆H₅) (17**).** Crystallization from CH₂Cl₂/pentane; ¹H NMR (400 MHz, CDCl₃) δ 7.50 (br s, 1H), 7.32 (br s, 2H), 6.89–6.84 (m, 2H), 4.89 (br s, 1H), 4.52 (s, 1H), 4.45 (s, 1H), 4.25 (s, 5H), 3.21–3.18 (m, 1H), 1.98 (t, *J* = 7.6 Hz, 3H), 1.66 (d, *J* = 12.2 Hz, 9H), 1.18 (d, *J* = 12.0 Hz, 9H), 2.63–0.86 (m, 22H); ³¹P NMR (162 MHz, CDCl₃) δ 73.51 (d, *J* = 36.6 Hz), 18.21 (br s); HRMS *m/z*: calcd for C₃₈H₅₇FeP₂Pd 737.2320, found 737.2328.

Pd(CyPF-*t*-Bu)(Br)(4-ClC₆H₄) (18**).** Crystallization from CH₂Cl₂/pentane; ¹H NMR (400 MHz, CDCl₃) δ 7.11 (d, *J* = 8.3 Hz, 2H), 6.89 (d, *J* = 7.8 Hz, 2H), 4.88 (br s, 1H), 4.53 (s, 1H), 4.47 (s, 1H), 4.25 (s, 5H), 3.19–3.16 (m, 1H), 1.98 (t, *J* = 7.6 Hz, 3H), 1.67 (d, *J* = 11.7 Hz, 9H), 1.18 (d, *J* = 13.2 Hz, 9H), 2.51–0.86 (m, 22H); ³¹P NMR (162 MHz, CDCl₃) δ 75.03 (d, *J* = 33.5 Hz), 18.44 (br s); HRMS *m/z*: calcd for C₃₈H₅₆ClFeP₂Pd 771.1930, found 771.1925.

Pd(CyPF-*t*-Bu)(Br)(4-CF₃C₆H₄) (19**).** Crystallization from CH₂Cl₂/pentane; ¹H NMR (400 MHz, CDCl₃) δ 7.35 (d, *J* = 7.8 Hz, 2H), 7.12 (d, *J* = 7.8 Hz, 2H), 4.89 (br s, 1H), 4.54 (s, 1H), 4.48 (s, 1H), 4.26 (s, 5H), 3.19–3.17 (m, 1H), 1.99 (t, *J* = 7.4 Hz, 3H), 1.66 (d, *J* = 12.7 Hz, 9H), 1.18 (d, *J* = 13.2 Hz, 9H), 2.69–0.87 (m, 22H); ³¹P NMR (162 MHz, CDCl₃) δ 77.56 (d, *J* = 32.6 Hz), 20.67 (br s); HRMS *m/z*: calcd for C₃₉H₅₆F₃FeP₂Pd 805.2194, found 805.2206.

Pd(D-*t*-BPF)(4-MeO₂CC₆H₄)(BF₄) (20**).** AgBF₄ (0.91 mmol) in THF (5 mL) was added to a solution of Pd(D-*t*-BPF)(Br)(4-MeO₂CC₆H₄) (0.70 mmol) in CH₂Cl₂ (35 mL). The suspension was stirred at room temperature for 1 h. The product was isolated by filtration. Recrystallization from THF gave brown needles (89%). ¹H NMR (400 MHz, CDCl₃) δ 7.82 (d, *J* = 7.8 Hz, 2H), 7.78 (d, *J* = 7.8 Hz, 2H), 5.41 (s, 4H), 4.30 (s, 4H), 3.92 (s, 3H), 1.39 (t, *J* = 7.3 Hz, 18H), 1.37 (d, *J* = 7.4 Hz, 18H); ³¹P NMR (162 MHz, CDCl₃) δ 21.27; ¹¹B NMR (128 MHz, CDCl₃) δ 6.50; HRMS *m/z*: calcd for C₃₄H₅₁FeO₂P₂Pd 715.1749, found 715.1755. The X-ray structure is shown in Scheme 6.

Kinetic Measurement of Coupling between Potassium Allyltrifluoroborates and *p*-Substituted Bromoarenes (Scheme 3). To a solution of Pd(OAc)₂ (0.015 mmol), D-*t*-BPF (0.018 mmol), potassium (*E*)-2-butenyltrifluoroborate (0.75 mmol), and K₂CO₃ (1.5 mmol) in THF (7 mL) was added *p*-substituted bromoarene (0.5 mmol) (*p*-PhOC₆H₄Br, *p*-MeC₆H₄Br, PhBr, *p*-ClC₆H₄Br, or *p*-CF₃C₆H₄Br). The mixture was stirred at 75 °C. The reaction progress was followed by gas chromatography (GC) analysis of the coupling product.

Competitive Reactions Using Pd(D-*t*-BPF)(Ar)(Br) or Pd(CyPF-*t*-Bu)(Ar)(Br) (Schemes 4 and 5). A 20 mL flask was charged with Pd(D-*t*-BPF)(Ph)(Br) (0.25 mmol), Pd(D-*t*-BPF)(Ar)(Br) (0.25 mmol Ar = *p*-PhOC₆H₄, *p*-ClC₆H₄, *p*-CF₃C₆H₄), potassium (*E*)-2-butenyltrifluoroborate (0.75 mmol), and K₂CO₃ (1.5 mmol) under nitrogen. THF (7 mL) was added, and the resulting

(35) Ukai, T.; Kawazura, H.; Ishii, Y.; Bonnet, J. J.; Ibers, J. A. *J. Organomet. Chem.* **1974**, *65*, 253.

(36) (a) Paul, F.; Patt, J.; Hartwig, J. F. *Organometallics* **1995**, *14*, 3030. (b) Widenhoefer, R. A.; Zhong, H. A.; Buchwald, S. L. *Organometallics* **1996**, *15*, 2745.

(37) Roy, A. H.; Hartwig, J. F. *J. Am. Chem. Soc.* **2003**, *125*, 8704.

(38) (a) Lee, C.; Parr, R. G.; Yang, W. *Phys. Rev. B* **1988**, *37*, 785. (b) Becke, A. D. *J. Chem. Phys.* **1993**, *98*, 5648. (c) Stephens, P. J.; Devlin, F. J.; Chabalowski, C. F.; Frisch, M. J. *J. Phys. Chem.* **1994**, *98*, 11623.

(39) Frisch, M. J.; Trucks, G. W.; Schlegel, H. B.; Scuseria, G. E.; Robb, M. A.; Cheeseman, J. R.; Montgomery, J. A., Jr.; Vreven, T.; Kudin, K. N.; Burant, J. C.; Millam, J. M.; Iyengar, S. S.; Tomasi, J.; Barone, V.; Mennucci, B.; Cossi, M.; Scalmani, G.; Rega, N.; Petersson, G. A.; Nakatsuji, H.; Hada, M.; Ehara, M.; Toyota, K.; Fukuda, R.; Hasegawa, J.; Ishida, M.; Nakajima, T.; Honda, Y.; Kitao, O.; Nakai, H.; Klene, M.; Li, X.; Knox, J. E.; Hratchian, H. P.; Cross, J. B.; Adamo, C.; Jaramillo, J.; Gomperts, R.; Stratmann, R. E.; Yazyev, O.; Austin, A. J.; Cammi, R.; Pomelli, C.; Ochterski, J. W.; Ayala, P. Y.; Morokuma, K.; Voth, G. A.; Salvador, P.; Dannenberg, J. J.; Zakrzewski, V. G.; Dapprich, S.; Daniels, A. D.; Strain, M. C.; Farkas, O.; Malick, D. K.; Rabuck, A. D.; Raghavachari, K.; Foresman, J. B.; Ortiz, J. V.; Cui, Q.; Baboul, A. G.; Clifford, S.; Cioslowski, J.; Stefanov, B. B.; Liu, G.; Liashenko, A.; Piskorz, P.; Komaromi, I.; Martin, R. L.; Fox, D. J.; Keith, T.; Al-Laham, M. A.; Peng, C. Y.; Nanayakkara, A.; Challacombe, M.; Gill, P. M. W.; Johnson, B.; Chen, W.; Wong, M. W.; Gonzalez, C.; Pople, J. A. *Gaussian 03*, revision B.04; Gaussian, Inc.: Pittsburgh, PA, 2003.

solution was heated to 75 °C. The relative rate was estimated by GC analysis of coupling products (a sum of products **6** and **7**).

Computational Details. All calculations were performed by means of the density functional theory method, the hybrid Becke3LYP functional with a hybrid Becke exchange functional, and a Lee–Yang–Parr correlation functional as implemented in Gaussian 03.^{39,40} The basis sets were described using an effective core potential (LANL2DZ) for all atoms.⁴¹ The structures at the stationary points were fully optimized at the B3LYP/LANL2DZ level of theory. Solvent effects on the energy diagram were included using self-consistent reaction field (SCRF) method using CPCM.⁴² Tetrahydrofuran (THF) was used as solvent throughout.

(40) (a) Wadt, W. R.; Hay, P. J. *J. Chem. Phys.* **1985**, *82*, 284. (b) Hay, P. J.; Wadt, W. R. *J. Chem. Phys.* **1985**, *82*, 299.

Acknowledgment. This work was supported by a Grant-in-Aid for Scientific Research in Priority Areas (no. 18064001, Synergy of Elements) and the Global COE Program (No. B01, Catalysis as the Basis for Innovation in Materials Science) from the Ministry of Education, Culture, Sports, Science, and Technology, Japan.

Supporting Information Available: Text describing experimental details, spectral and analytical data of the products, and X-ray data (PDF). This material is available free of charge via Internet at <http://pubs.acs.org>.

OM800832R

(41) (a) Barone, V.; Cossi, M. *J. Phys. Chem. A* **1998**, *102*, 1995. (b) Cossi, M.; Scalmani, G.; Rega, N.; Barone, V. *J. Comput. Chem.* **2003**, *24*, 669.